

BIO-INSPIRED SYNTHESIS OF BARIUM PHOSPHATES NANOPARTICLES AND ITS CHARACTERIZATION

X. N. YU^{a, b}, C. X. QIAN^{a, b*}, X. WANG^{a, b}

^a*School of Materials Science and Engineering, Southeast University, Nanjing 211189, China*

^b*Research Institute of Green Construction Materials, Southeast University, Nanjing 211189, China*

Nano-sized barium phosphates were prepared under different pH values in the centrifuged solution of substrate and bacteria. The structural characterization by fourier transform infrared spectroscopy (FTIR), X-ray techniques (XRD) and morphological observations via scanning electron microscope (SEM) and transmission electron microscopy (TEM) showed that the nanostructures of barium phosphates were prepared. And thermal properties of BaHPO₄ nanoparticles were investigated at pH=8 by thermogravimetric-differential scanning calorimetry (DSC-TG) analysis. Powder XRD patterns furnished evidence for the formation of barium phosphates having average crystallite size 48.56, 36.60, 31.89, 33.27 and 34.79nm which precipitated in the centrifuged solution under different pH values. TEM images indicate that all barium phosphates nanoparticles are irregular flakes in shape with sizes in the range of 20-100nm.

(Received January 21, 2015; Accepted March 6, 2015)

Keywords: Barium phosphates, Nanoparticles, Structural, X-ray techniques, Thermal properties

1. Introduction

Various sophisticated nanostructures with unique properties have been generated through a natural biomineralization process in recent years [1-4]. In particular, functional nanomaterials such as battery (LiFePO₄/C) have been synthesized under the assistance of organic matrix as structural templates [5]. A specific set of organic matrix, including proteins, poly-saccharides, proteolipids, and proteoglycans, can regulate nucleation, growth, size, and orientation of the crystals [6]. The principal process is organic matrix and inorganic ions interact in the interphase which enables the biogenic mineral to have the special multistage structure and assembly regulating inorganic mineral face separated from molecular horizontal [7]. A key feature common to all biomineralizing systems is their dependency upon the biosynthesis of an extracellular organic matrix that is competent to direct the formation of the subsequent mineral phase [8]. In recent years, bacteria and biomacromolecules, which have been used as a new class of additives to control the morphology and size of inorganic crystals, such as Fe₃O₄ or Fe₃S₄ [9, 10], CaCO₃ [11, 12], SiO₂ [13], LiFePO₄/C [5] and so on.

The alkaline earth phosphates (such as barium phosphates) have been extensively studied in the past years for their applications in different fields such as bioceramics, ionic conductivity, ferroelectrics, luminescence, metal-doped and corrosion resistance, etc [14-17]. There are a lot of

*Corresponding author: cxqian@seu.edu.cn

synthetic process to prepare barium phosphates, including gel method [18, 19], electrochemical technique [20], hydrothermal synthesis [21], high-temperature solid-state method [22], and chemical precipitation [23-25]. From all these methods, the desired material can be obtained in single crystals and powder form in bulk. But a few investigations are focus on the syntheses of nanostructures of barium phosphates via biological deposition. In this research, *B. subtilis* was selected as the suitable microorganism, which could produce alkaline phosphatase (EC 3.1.3.1) constantly hydrolyzed phosphate monoester by enzymolysis in bacterial solution, and then PO_4^{3-} or HPO_4^{2-} was obtained. In this circular process, PO_4^{3-} or HPO_4^{2-} concentration in solution is increasing with the continuous decompositions of substrate. MHPO_4 , MPO_4 , $\text{M}_3(\text{PO}_4)_2$ and so on can be prepared by phosphate ions reacting with metal cations.

2. Experimental

All raw materials were of analytically pure grade and used without further purification. And deionized water was self-made.

B. subtilis cultivation: 3g beef extract, 5g typtone, 1.5g NaCl were completely dissolved in 1L of deionized water, and its pH value was adjusted to 7.0 using diluted NaOH solution. Next, 1L of mixture solution was added to ten bottles (250ml), and each bottle were wrapped by employing gauze and paper. Ten bottles were placed in autoclave under $125\pm 2^\circ\text{C}$ and 0.1Mpa conditions for 25 ± 2 min. As a result, 3mL of liquid strains was added to each bottle and cultivated in the oscillation incubator ($170\text{r}\cdot\text{min}^{-1}$) at $30\pm 2^\circ\text{C}$ for 24 h. In general, the harvested microorganisms were kept in a refrigerator at $4\pm 0.2^\circ\text{C}$ for stock prior to use. The bacterial liquid with an optical density (at 600 nm of wavelength) value of 1.69 and enzyme activity value of 0.23mmol/ (L min) was used in this study.

Syntheses of barium phosphates nanoparticles: a solution of substrate (1.25mol/l, 8ml) was injected into a 100ml solution of *B. subtilis*, and the mixed solution was allowed to stand under static conditions for 24h at $30\pm 2^\circ\text{C}$ in oven. After 24h, the mixed solution was centrifuged, obtained the supernatant. The solution was then adjusted to pH=7, 8, 9, 10 and 11. $\text{BaCl}_2\cdot 2\text{H}_2\text{O}$ (20mM) was added to the above solution of different pH values. And after 1 min of stirring, precipitated solution was stilled for 24h at room temperature. The products were filtrated and washed three times with deionized water and ethanol and then dried at $66\pm 2^\circ\text{C}$ for 24h. After that, all precipitates were collected and characterized.

Fourier transform infrared spectroscopy (FTIR) spectra of the samples were recorded using a Nicolet 5700 spectrometer by KBr pellet technique in the range of $399\text{--}4000\text{ cm}^{-1}$. The phase purity of products was examined by powder XRD with Bruker D8-Discover diffractometer using graphite-monochromatized high-intensity Cu K α radiation ($\lambda=1.5406\text{\AA}$). The surface morphology was observed using a scanning electron microscope (SEM, FEI Company, Netherlands, operating voltage 20 kV). Transmission electron microscopy (TEM) images were obtained on a FEI, G2 20 equipment. TEM grids were prepared using a few drops of nanoparticles followed by drying. DSC-TG were carried out on STA449 F3 thermogravimetric analyzer (Netzsch, Germany). The analyses were carried out simultaneously in a nitrogen atmosphere at a heating rate of $10^\circ\text{C} / \text{minute}$ between room temperature and 700°C .

3. Results and discussion

The FTIR spectrum was effectively used to identify the functional groups of the samples. The FTIR spectra of barium phosphates obtained at pH=8 is displayed in Figure 1a. At room temperature the strong and broad band at 3415.62 cm^{-1} is due to KBr mull absorption, which appears in the spectrum of any compound. A shoulder band at 2973.47 cm^{-1} is corresponds to hinder rotation. The peak at 2443.95 cm^{-1} may result from the rotational band. The peaks at 1650.24 cm^{-1} which reveals thermal vibrations of H^+ ions in an intermolecular phonon vibration associated with $\text{H}^+\text{-PO}_4^{3-}$ contacts. The vibrational absorptions at 1391.75 , 1076.58 and 982.25 cm^{-1} are corresponding to stretching vibrations of P-O (H). The P=O stretching vibration leads to a distinct band at 1258.78 cm^{-1} . The P=O deformation vibration is found at 892.04 cm^{-1} , which is non-degenerate. The P-O(H) wagging and rocking vibrational bands are noticed at 537.45 cm^{-1} . The above results are similar with literatures reported [16, 26]. The IR spectrum exhibits broad peaks at 3411.74 , 1645.18 , 1403.90 , 1017.95 , 870.66 and 566.45 cm^{-1} with respect to the OH and PO_4^{3-} in the Figure 1b. And the observed wave numbers, relative intensities obtained from the recorded spectra and the assignments proposed for the title compounds were given in accordance with the data reported in the literature [19].

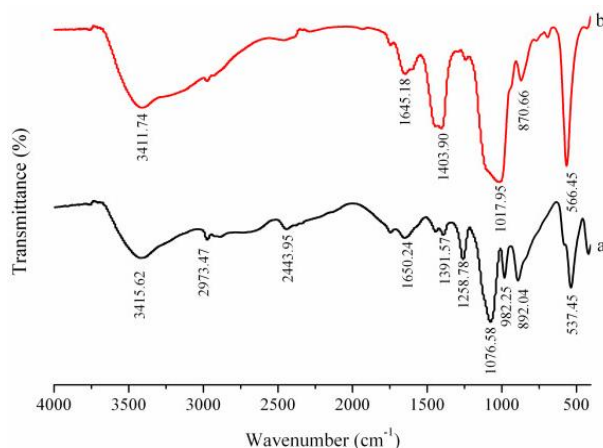


Fig. 1. FTIR spectrum of barium phosphates nanoparticles obtained at pH=8 (a) and 11 (b).

XRD patterns of barium phosphates are shown in Figure 2. Barium phosphates patterns can be readily indexed to the reported structures of BaHPO_4 JCPDS Card No. 72-1370 (Figure 2a, b, c) when $\text{pH}<10$, and no peaks attributable to impurities are observed (Figure 2 a, b, c). However, it is to be noted that the products are mainly mixture precipitated in the centrifuged solution of substrate with bacteria when $\text{pH}=10$ and 11 are shown in Figure 2d, e. The mixture of BaNaPO_4 , BaHPO_4 and $\text{Ba}_5(\text{PO}_4)_3\text{OH}$ (JCPDS No. 70-1787, 09-0113 and 36-0272) is found when $\text{pH}=10$ (Figure 2d). The mixture of BaNaPO_4 and $\text{Ba}_5(\text{PO}_4)_3\text{OH}$ precipitated in the centrifuged solution of substrate with bacteria when $\text{pH}=11$ (Figure 2e). The standard XRD patterns of the reported structures of BaNaPO_4 and $\text{Ba}_5(\text{PO}_4)_3\text{OH}$ used are JCPDS No. 70-1787 and 78-1441, respectively (Figure 2e). The above results imply that phosphate ions are in the form of HPO_4^{2-} when $\text{pH}=7, 8, 9$, HPO_4^{2-} and PO_4^{3-} when $\text{pH}=10$, and PO_4^{3-} when $\text{pH}=11$ in the centrifuged solution of substrate with bacteria. The results of X-ray diffraction (XRD) indicate

that the samples are mainly BaHPO_4 when $\text{pH} < 10$. By calculating the distribution coefficients of $[\text{HPO}_4^{2-}]$, it is easy to explain that BaHPO_4 was the main precipitate when $\text{pH} < 10$ [27]. However, the distribution coefficients of $[\text{PO}_4^{3-}]$ could neglect in theory compare to the distribution coefficients of $[\text{HPO}_4^{2-}]$ when $\text{pH} = 10$ and 11, but the distribution coefficients of $[\text{PO}_4^{3-}]$ can not ignored in fact [27]. It is easy to conclude that *B. subtilis* can produce a specific enzyme constantly hydrolyze phosphate monoester in mixed solution of substrate and bacteria, and $\text{PO}_4^{3-}/\text{HPO}_4^{2-}$ ions are then obtained.

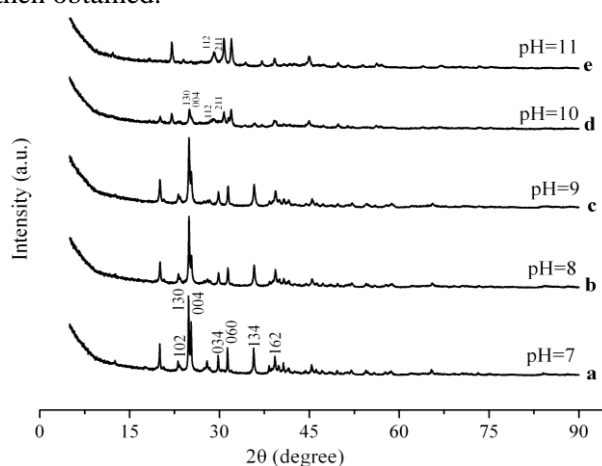
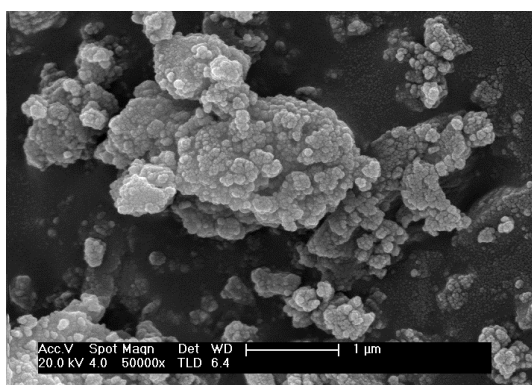
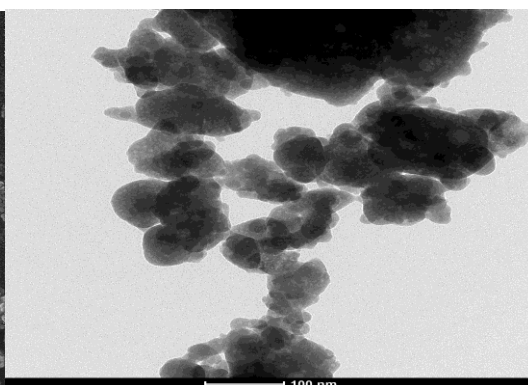


Fig. 2. XRD patterns of barium phosphates precipitated in the centrifuged solution of substrate and bacteria (Figure 2a, b, c, d, e).

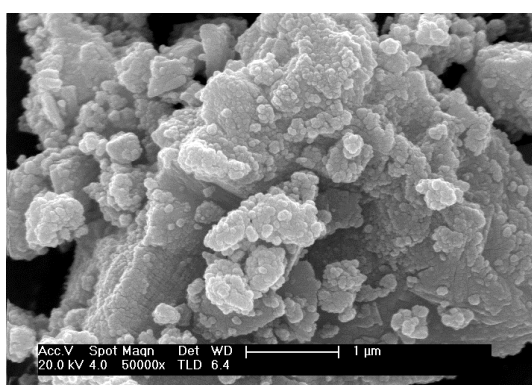
Fig. 3 shows SEM (Fig. 3 a, c, e, g, i) and TEM (Figure 3 b, d, f, h, j) images of barium phosphates nanoparticles. SEM images show that all barium phosphates are nano-agglomerates, as shown in Figure 3 a, c, e, g, i. The size of the nano-agglomerates is not uniform; the diameter is less than $3\mu\text{m}$. TEM images display that barium phosphates nanoparticles are mainly irregular flakes in shape with sizes in the range of 20-100nm (Figure 3 b, d, f, h, j). The average crystallite size of barium phosphates nanoparticles are estimated by the Scherrer formula [28], and the average size of nanoparticles are 48.56, 36.60, 31.89, 33.27 and 34.79nm when pH values are 7, 8, 9, 10 and 11, respectively. The results display that the barium phosphates nanoparticles are easily obtained by the centrifuged solution reacting with $\text{BaCl}_2 \cdot 2\text{H}_2\text{O}$, which are different from chemical and other biomineralization syntheses [23-25, 27].



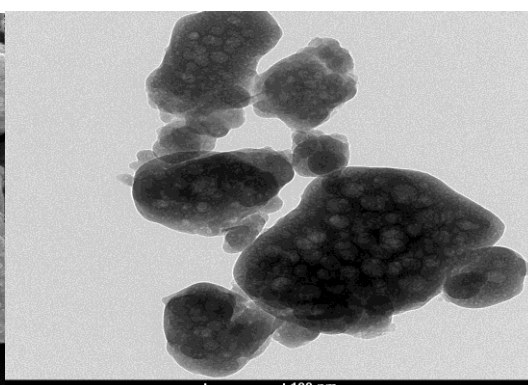
(a)



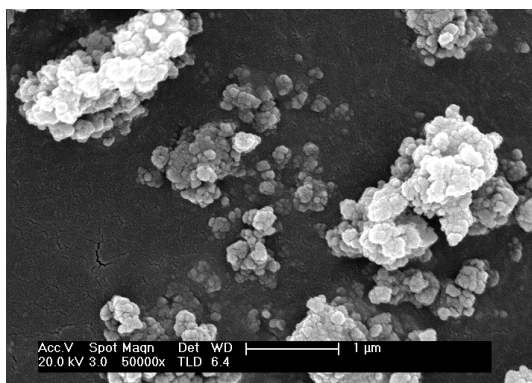
(b)



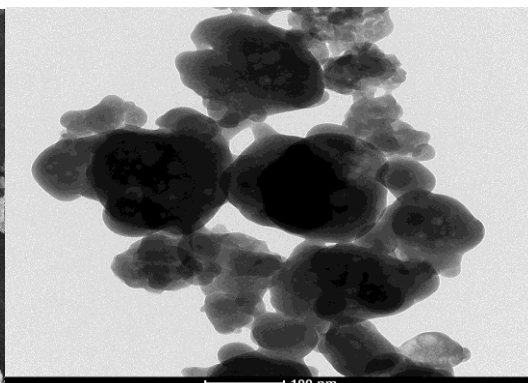
(c)



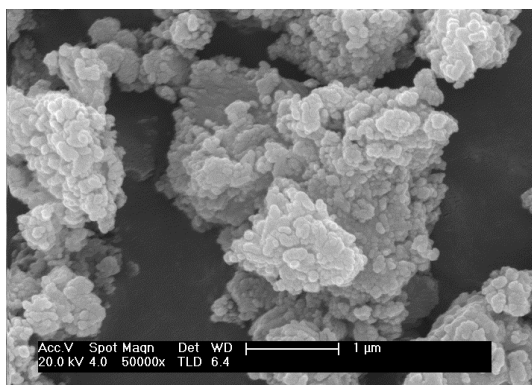
(d)



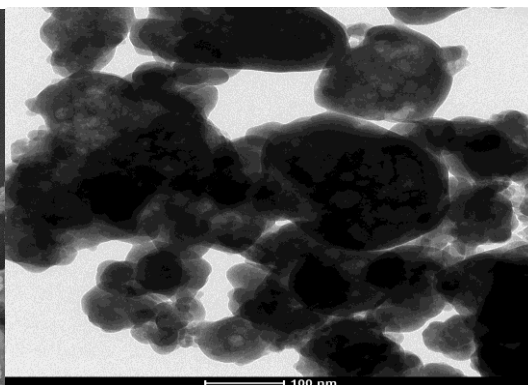
(e)



(f)



(g)



(h)

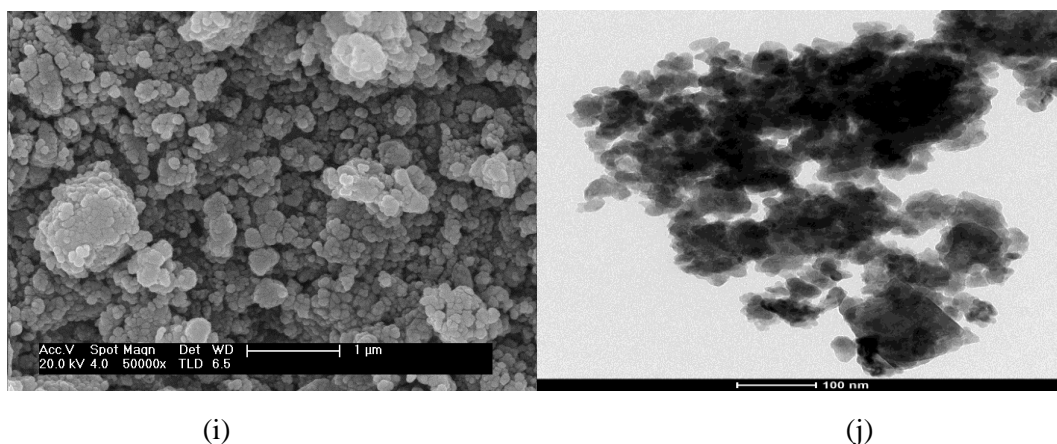


Fig. 3 SEM and TEM images of barium phosphates nanoparticles: (a, b), pH=7, (c, d), pH=8, (e, f), pH=9, (g, h), pH=10, (i, j), pH=11.

Fig. 4 shows the DSC-TG curves of BaHPO₄ nanoparticles at pH=8. From the results, it is observed that DSC curves show an endothermic peak at 447.5°C for nanoparticles. The peak at 447.5°C can be considered as the decomposition or melting points of the materials. From the results, it is noticed that BaHPO₄ nanoparticles have more thermal stability than other types of BaHPO₄ [21, 25]. The TG curve of BaHPO₄ nanoparticles displays that maximum weight loss occurs in the temperature range 420-460°C which is due to the decomposition of the samples.

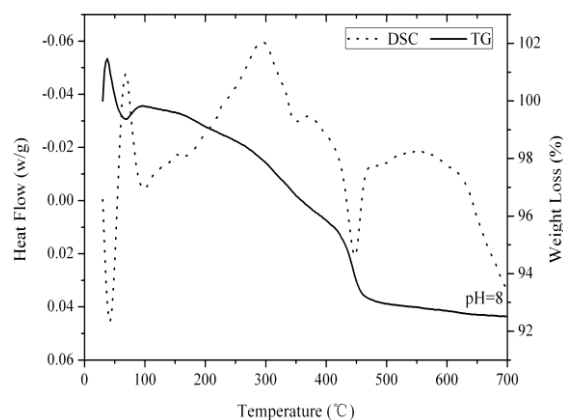


Fig. 4 DSC-TG curves of BaHPO₄ nanoparticles obtained at pH=8.

4. Conclusions

This work shows that barium phosphates nanoparticles can be obtained in the centrifuged solution of substrate with bacteria. By analyzing XRD results display that phosphate ions are in the form of HPO₄²⁻, HPO₄²⁻ and PO₄³⁻, PO₄³⁻ at different pH values of the centrifuged solution. Results of this research provide a new route to synthesize nanostructured barium phosphates in the centrifuged solution of substrate with bacteria under a certain pH values. And biomacromolecules in the centrifuged solution play an important role in the process of crystal nucleation, growth and accumulation of barium phosphates nanoparticles.

Acknowledgements

This work was supported by the National Nature Science Foundation of China (51372038), Scientific Research Foundation of Graduate School of Southeast University (YBJJ1453), and 333 Project of Jiangsu Province.

References

- [1] M. Mahmoudi, I. Lynch, M. R. Ejtehad, M. P. Monopoli, F. B. Bombelli, S. Laurent, *Chem. Rev.* **111**, 5610 (2011).
- [2] Y. Kong, F. Gao, R. He, J. Chen, X. Xu, N. Li, D. X. Cui, *Curr. Nanosci.* **6**, 446 (2010).
- [3] J. Chen, Y. F. Kong, J. J. Ji, J. Ruan, K. Wang, F. Gao, D. X. Cui, *Nanoscale* **4**, 4455 (2012).
- [4] Z. W. Chen, Z. H. Li, Y. H. Lin, M. L. Yin, J. S. Ren, X. G. Qu, *Biomaterials* **34**, 1364 (2013).
- [5] X. D. Zhang, W. He, Y.Z. Yue, R. M. Wang, J. X. Shen, S.J. Liu, J. Y. Ma, M. Li, F. X. Xua, *J. Mater. Chem.* **22**, 19948 (2012).
- [6] A. Veis, *Science* **307**, 1419 (2005).
- [7] S. Mann, *Nature* **332**, 119 (1988).
- [8] M. L. Paine, D. H. Zhu, W. Luo, P.B. Jr., M. Goldberg, S. N. White, Y. P. Lei, M. Sarikaya, H. K. Fong, M. L. Snead, *J. Struct. Biol.* **132**, 191 (2000).
- [9] D. Schüler, R. B. Frankel, *Appl. Microbiol. Biotechnol.* **52**, 464 (1999).
- [10] D. Schüler, E. Baeuerlein, *J. Bacteriol.* **180**,159 (1998).
- [11] G. Fu, S. Valiyaveetil, B. Wopenka, D. E. Morse, *Biomacromolecules* **6**,1289 (2005).
- [12] Y. F. Ma, L. Qiao, Q. L. Feng, *Mat. Sci. E. C* **32**,1963 (2012).
- [13] Y. Yao, D. Wang, L. Han, S. N. Che, *Chem. Eur. J.* **19**, 15489 (2013).
- [14] S. K. Arora, A. T. Oza, T. R. Trivedi, V. A. Patel, *Mat. Sci. E. B* **77**, 131 (2000).
- [15] T. R. Trivedi, A. T. Oza, V. A. Patel, S. K. Arora, *Cryst. Res. Technol.* **35**, 615 (2000).
- [16] D. Nallamuthu, P. Selvarajan, T. H. Freeda, *Physica B* **405**, 4908 (2010).
- [17] Y. G. Chen, B. L. Luan, G. L. Song, Q. Yang, D. M. Kingston, F. Bensebaa, *Surf. Coat. Tech.* **210**, 156 (2012).
- [18] K. C. Hebbar, S. M. Dharmaparakash, P. M. Rao, *J. Mater. Sci. Lett.* **10**, 1430 (1991).
- [19] M. Dinamani, P. V. Kamath, *Mater. Res. Bull.* **36**, 2043 (1997).
- [20] E. Banks, R. Chianel, *J. Appl. Cryst.* **7**, 301 (1974).
- [21] T. B. Chaabane, L. Smiri, A. Bulou, *Solid State Sci.* **6**, 197 (2004).
- [22] D. Y. Pan, D. R. Yuan, H. Q. Sun, S. Y. Guo, X. Q. Wang, X. L. Duan, C. N. Luan, Z. F. Li, *Cryst. Res. Technol.* **41**, 236 (2006).
- [23] C. Calvo, R. Faggiani, *Can. J. Chem.* **53**, 1849 (1975).
- [24] B. J. Boonchom, C. Ruttanapun, M. Thongkam, P. Chaiyasith, S. Woramongkonchai, S. Kongteweelert, N. Vittayakom, *Adv. Mater. Res.* **717**, 37 (2013).
- [25] H. A. Höpfe, M. Daub, O. Oeckler, *Solid State Sci.* **11**, 1484 (2009).
- [26] S. K. Arora, T. R. Trivedi, A. T. Oza, V. A. Patel, *Acta Mater.* **49**, 2103 (2001).
- [27] F. Wang, G. Y. Xu, Z. Q. Zhang, *Mater. Lett.* **59**, 808 (2005).
- [28] M. Rajkumar, N. M. Sundaram, V. Rajendran, *Dig. J. Nanomater. Bios.* **6**, 169 (2011).